

Article

# Mitigating the Load Frequency Fluctuations of Interconnected Power Systems Using Model Predictive Controller

Muhammad Majid Gulzar <sup>1,\*</sup>, Syed Tahir Hussain Rizvi <sup>2,\*</sup>, Muhammad Yaqoob Javed <sup>3</sup>, Daud Sibtain <sup>1</sup> and Rubab Salah ud Din <sup>1</sup>

<sup>1</sup> Department of Electrical Engineering, University of Central Punjab, Lahore 54782, Pakistan; daudsibtain@gmail.com (D.S.); rubab\_emaan@hotmail.com (R.S.u.D.)

<sup>2</sup> Department of Computer Engineering, The University of Lahore, Lahore 54000, Pakistan

<sup>3</sup> Department of Electrical and Computer Engineering, COMSATS University Islamabad, Lahore 54000, Pakistan; yaqoob.javed@cuiilahore.edu.pk

\* Correspondence: majid.gulzar@ucp.edu.pk (M.M.G.); tahir.hussain@dce.uol.edu.pk (S.T.H.R.); Tel.: +92-335-411-2293 (M.M.G.)

Received: 31 October 2018; Accepted: 14 January 2019; Published: 1 February 2019



**Abstract:** The penetration of renewable energy sources into the conventional power systems are evolving day by day. Therefore, in this paper, a photovoltaic (PV) connected thermal system is discussed and analyzed by keeping PV to operate at maximum power point (MPP). The main problem in the interconnection of these systems is load frequency fluctuations due to different load changing conditions. The model predictive controller (MPC) has the ability to predict the target value at real-time with fast convergence. Therefore, MPC is proposed to negate this problem by giving minimum oscillation. The comparison analysis is carried out with other conventional controllers, including genetic algorithm-based PI, firefly algorithm-based PI and PI controller. Simulation results clearly exhibit the outclass performance of MPC over all other controllers.

**Keywords:** load frequency control; thermal system; photovoltaic; maximum power point; model predictive controller

## 1. Introduction

Renewable resources play an essential role in achieving energy demand. Almost 18% of the world energy demand is fulfilled through renewable resources [1]. The trend is now moving toward the renewable resources due to the depletion of fossil fuels. However, it is very challenging to meet certain requirements of voltage and current for the power systems. Among the renewable energy resources, the solar photovoltaic (PV) system is the most widely used technology in the power system, so the diffusion of PV into the power system has a major effect on the frequency and voltage of the system. Moreover, when the system frequency remains stable throughout the process, this indicates the load is balanced. The variation in load directly affects the frequency and causes it to deviate from its nominal value [2]. Therefore, the penetration of renewable energy resources output to the grid should have, minimum fluctuations in frequency [3,4]. Furthermore, the performance of the electrical power system will deteriorate with the load fluctuation, fault, rapid change in the load, and operational uncertainty, etc.

Power systems are composed of several interconnected areas and each area is interlinked to another area via a transmission line (tie-line). In a single area, several thermal generators are connected with a group of renewable energy sources to fulfill its own energy demands and manage power exchange with nearby areas. However, due to the variations in the generation and the load, the voltage

and frequency of the power system deviate from its limits. The power system, which is used in this research article, contains solar PV and thermal energy generators.

The PV system is the fastest growing and most widely used renewable energy source because it is a pollution-free, environmentally friendly, and noise-free source of energy. In 2017, the solar PV produced more than 402 GW of electricity [5]. The PV system provides a DC output and is connected via grid in three stages [6]. The first stage is the DC-to-DC converter stage, which adjusts the voltage at the desired level. The second stage is the inverter, which converts the DC into AC output, which is compatible with the grid. In the final stage, the output of the inverter is given to the power grid. The connection of PV array to the grid is controlled with the help of the DC-AC inverter. The efficiency of the system is dependent on the DC-to-DC converter because it makes the system operate at the maximum power point (MPP). However, the thermal unit consists of a governor, steam turbine, re-heater, generator, and droop. The thermal power system is controlled through automatic generation control (AGC), which has two controllable parts: The automatic voltage regulator (AVR) and the load frequency control (LFC) [7].

This paper focuses on LFC, rather than AVR, because load change has a greater effect on the frequency than the voltage. Moreover, in an interconnected system, the frequency effect is more prominent than the voltage. In the electrical power system, the nature of the loads is irregular and unpredictable. The difference in generation or abnormality in a system leads to a mismatch in frequency, and the scheduled power between these areas deteriorates. Therefore, the LFC mechanism is used to maintain the frequency within the required limit. Thus, LFC plays a substantial role in improving the operation of the power system. Due to growing interest in the field of LFC, multiple control methods have been introduced by the researchers in order to mitigate the frequency fluctuation problem. Various control techniques, like the classical control technique, adaptive control technique, optimal control technique, and the robust control technique are used. Commonly used methods, such as proportional-integral-derivative (PID) [8] and sliding-mode control [9], were previously introduced for centralized systems, but were not feasible for the large-scale area. Furthermore, many soft computing techniques were used by researchers, such as artificial neural networks (ANN) [10,11] and fuzzy logic control (FLC) [12,13]. These algorithms have the ability to deal effectively with non-linearity of the power system, but demand excessive training and extensive hard work to compute influential signal. Many evolutionary soft computing techniques were previously proposed to solve the LFC problem, such as genetic algorithm (GA) [14,15], particle swarm optimization (PSO) [16], gravitational search [6], ant colony method (ANM) [17], firefly (FA) [18], cuckoo search algorithm [19], and bat algorithm [20]. These techniques seem to work effectively for LFC problem, but still are unable to minimize the frequency fluctuation issue.

Recently, MPC-based applications on LFC problem were introduced [21], but most of the work was carried out on single/multi-area for similar conventional sources, i.e. the thermal unit. The trend of utilizing the renewable sources is evolving, and penetration of renewable sources into the conventional power systems has a major effect on the overall power generation system. Therefore, it is necessary to introduce a controller, which has the ability to work with the increasing challenges in a power system to solve the frequency fluctuation problem. This paper highlights the PV tie thermal unit for single/multi-area and checks its response with the change in load, or imbalance, between these areas. Motivation to cater this problem for the single/multi-area system originated from the specifications of MPC in view (fast convergence, robustness, and fast response). This paper sheds the light on the impact of frequency fluctuation with load change for the interconnected power system. The proposed MPC-based technique clearly demonstrates its ability to track and predict the future values to make sure the system remains under less disturbance and could achieve its target under less possible time without showing much disturbance.

This paper is organized as follows: Section 2 is related to the model of an interconnected power system, Section 3 illustrates the details of the proposed MPC based on LFC problem. In Section 4,

the simulation and results of the proposed solution are shown. Finally, the conclusion is shown in Section 5.

## 2. Models for Interconnected Power Systems

The single-area contains a PV and thermal unit, while two-area consists of two units each (PV and thermal). The modeling of these systems is demonstrated in the following sections.

### 2.1. Thermal Generator Model

The thermal generation model consists of a generator, steam turbine, governor, re-heater, and droop. Governor is used to control the speed of the turbine based on the error that is introduced due to the change in power and frequency ( $\Delta P-\Delta f$ ). Furthermore, the governor controls the mechanical motion of the turbine by controlling the operation of the valve and by regaining the lost energy after passing through re-heater, which helps to achieve the required target [22]. The droop is used to control the speed of prime-mover, which is connected with the generator. The last unit is the generator in a thermal power system, which converts the mechanical motion into electricity, which is our basic requirement. The parameters for the thermal unit, including time and gain constants, are given in Table 1 with their particular values.

Table 1. Parameters for thermal unit.

Parameter	Definition	Value
R	Droop	2.4 pu/Hz
$K_p$	Gain constant	120
$K_r$	Re-heater gain	0.5
$T_p$	Generator time-constant	20 s
$T_r$	Re-heater time-constant	10 s
$T_t$	Turbine time-constant	0.3 s
$T_g$	Governor time-constant	0.08 s

Moreover, the transfer functions of the thermal unit associated with the parameters are listed in Table 2 [23].

Table 2. Transfer function for components of thermal unit.

Component	Transfer Function
Governor	$G_G(s) = \frac{\Delta P_G(s)}{\Delta P_C(s)} = \frac{1}{(T_g s + 1)}$
Steam turbine	$G_T(s) = \frac{\Delta P_T(s)}{\Delta P_V(s)} = \frac{1}{T_t s + 1}$
Re-heater	$G_R(s) = \frac{\Delta P_R(s)}{\Delta P_T(s)} = \frac{K_r T_r s + 1}{T_r s + 1}$
Generator	$G_{Gen}(s) = \frac{\Delta F(s)}{\Delta P_M(s)} = \frac{K_p}{T_p s + 1}$
Droop	$G_D(s) = \frac{\Delta P_D(s)}{\Delta F(s)} = \frac{1}{R}$

The parameters for single/two-area are the same, but in the case of two-area, a bias factor is introduced with a tie line, which indicates the amount of power transferred between the two areas.

### 2.2. Photovoltaic Modeling

One of the most widely used renewable sources of energy is the PV system. It has a current source with a diode in parallel, making it a non-linear current source, which directly converts the solar irradiation into electricity by diffusing the motion of electron and holes within the PV cell. As it is a non-linear current source, it is essential to form the PV source to always operate on its MPPT so that maximum power can be attained [24].

Figure 1 illustrates the I-V curve characteristics at 25 °C. As irradiance decrease from 1000 W/m<sup>2</sup> to 100 W/m<sup>2</sup>, the I<sub>PV</sub> also decrease accordingly. At 500 W/m<sup>2</sup>, the current is half of its full value, while there is a little effect on voltage V<sub>PV</sub>. In this paper, the PV for the interconnected system is considered to operate at MPPT, at 1000 W/m<sup>2</sup> at 25 °C.

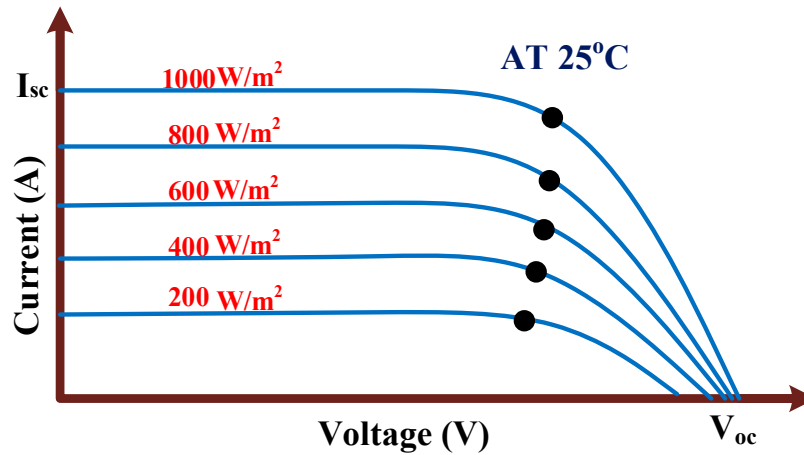


Figure 1. Current-voltage characteristic of the photovoltaic (PV).

AC voltage can be calculated using Equation (1)

$$m = \frac{V_{DC}}{V_{AC}} \tag{1}$$

where  $m$  is the gain between the AC and DC voltage in the system and its value is generally less than 0.86. For this model, its value is 0.7.

The transfer function of the boost converter can be calculated using Equations (2) and (3).

$$M_1 = \frac{V_2}{V_1} = \frac{I_1}{I_2} \tag{2}$$

$$G_1(s) = \frac{1}{M_1} \tag{3}$$

where  $1/M_1$  is the gain of the boost converter. The transfer function of the inverter is mentioned in Equation (4)

$$G_2(s) = \frac{i_{AC}(s)}{i_2(s)} = \frac{s^2}{s^2 + w^2} \tag{4}$$

Here,  $w = 2\pi f = 2\pi(50) = 314.12$  rad/sec. For instantaneous power, the transfer function is given in Equation (5), where  $\frac{V_m}{I_m}$  is the impedance

$$P(s) = \frac{V_m I_m}{2s} + \frac{V_m I_m}{2} \frac{s}{s^2 + (2w)^2} \tag{5}$$

The gain in instantaneous power is mentioned in Equation (6)

$$G_3(s) = \frac{P(s)}{i_{AC}(s)} = V_m \left( \frac{(s^2 + w^2)(s^2 + (2w)^2)}{s^2(s^2 + (4w)^2)} \right) \tag{6}$$

The Laplace domain equation for average power is given in Equation (7)

$$P_{avg}(s) = \frac{V_m I_m}{2s} \tag{7}$$

The gain for average power is shown in Equation (8)

$$G_4(s) = \frac{P_{avg}(s)}{P(s)} \tag{8}$$

### 3. Model Predictive Controller

MPC is an advanced method used by many researchers to satisfy a number of constraints dealing with the non-linear, as well as the linear, system having disturbances. It consists of three blocks, process model, controller, and a filter [25]. The process model is a key block for the success of MPC and it predicts the real-time values of output variables. Moreover, it is used to design the multi-input/output systems and satisfy all sorts of constraints [26]. The main objective of MPC is to prevent excessive movement in the input variable, to control the input/output constraints, and to process variables to find the optimal value within the specified range [27]. MPC is also used in controlling the switching of an inverter on the bases of the input voltage and current.

Figure 2 represents the dynamic model for a thermal connected PV system. The model is designed on the basis of an actual model of the conventional power system. Considering the actual model, the thermal and PV area are designed, where the PV area has to meet certain demands (voltage and frequency) to be integrated with a thermal section. In the designing of the PV area, it is considered that PV is operating at MPP, which not only eases the calculation, but also leads to less frequency deviation in thermal power system because of the nature of DC output. Furthermore, the thermal section contains the required units (governor, turbine, re-heater, and generator). The control section is installed in the thermal section because the load has a major effect on the thermal section, where a change in frequency is not desirable.

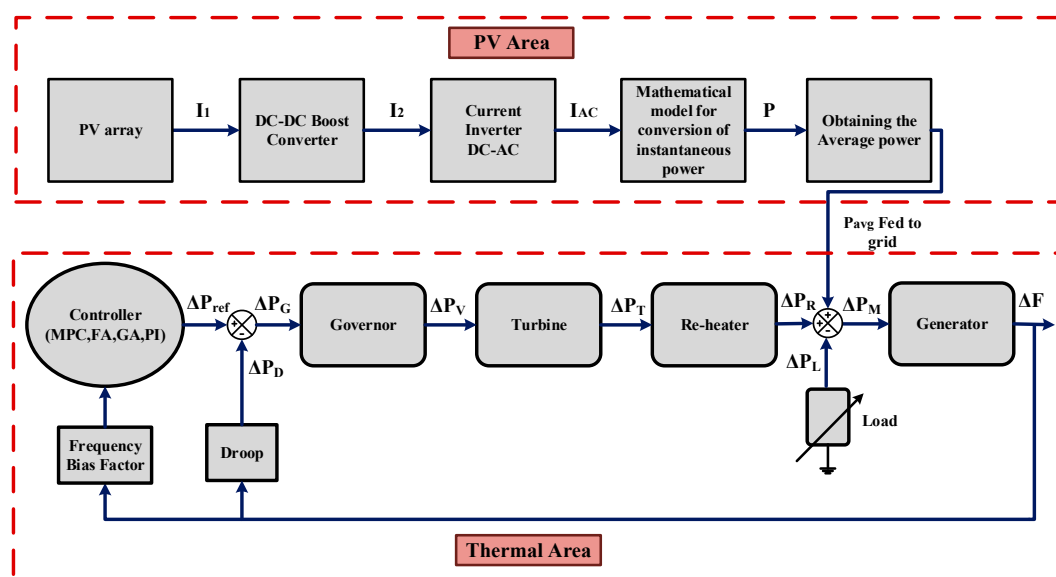


Figure 2. Dynamic model for the PV-thermal interconnected system.

Figure 3 shows the MPC structure, in which the internal model predicts the plant future output based on the past experience and recent values of input and output for the optimal future control actions. The prediction is composed of free and forced responses. The free response gives the expected output while considering the future control at zero, whereas the forced response adds the output response on the basis of future control that is generated by optimization block, which constitutes the minimizing cost function and hard constraints. The future error, or predicted error, is originated from the reference trajectory and the total response.

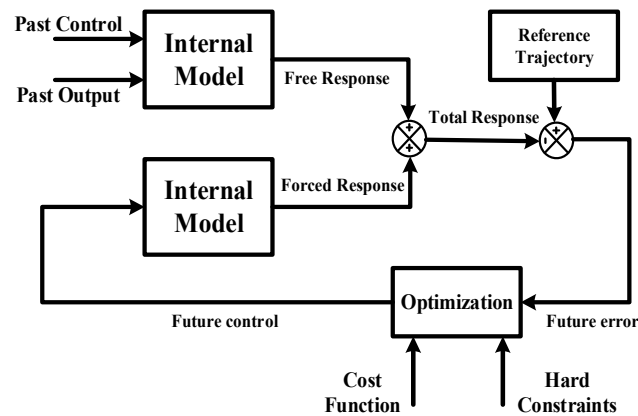


Figure 3. Block diagram of the model predictive controller (MPC).

The MPC is installed to mitigate the LFC problem for the PV connected thermal system. MPC optimization equation is constructed to tighten the future output error to zero. To demonstrate the MPC control calculations the quadratic cost function ( $J$ ) is defined in Equation (9)

$$J(N_1, N_2, N_u) = \sum_{j=N_1}^{N_2} \alpha(j) [\hat{Y}(k+j|k) - w(k+j)]^2 + \sum_{j=1}^{N_u} \beta(j) [u(k+j-1)]^2 \quad (9)$$

where  $N_1$ ,  $N_2$  are the lower and upper prediction horizons over the output, and  $N_u$  is the control horizon, where  $\alpha(j)$  and  $\beta(j)$  are the weights.  $w(k+j)$  represents the reference trajectory over a future horizon and  $u(k+j)$  calculates the future control.  $\hat{Y}(k+j|k)$  is the total response, which represents the sum of forced and free responses.

The predictive control law of MPC is based on prediction error, rather than control error (set-measured)

$$\hat{E}(k+1) \triangleq Yr(k+1) - \hat{Y}(k+1) \quad (10)$$

$Yr(k+1)$  is the corrected prediction and  $\hat{E}(k+1)$  predicts a uniform error vector.

$$\tilde{E}(k+1) \triangleq Yr(k+1) - \hat{Y}(k+1) \quad (11)$$

$\tilde{E}(k+1)$  is the deviation from the reference trajectory and  $\hat{Y}(k+1)$  is the unforced case and is defined by Equation (12)

$$\hat{Y}(k+1) \triangleq \hat{Y}(k+1) + I[y(k) - \hat{y}(k)] \quad (12)$$

where  $k+1$  is the sampling instant of the prediction horizons. The equality constraint equation of MPC,  $u$  and  $\Delta u$ , defines the lower and upper limits

$$u - (k) \leq k+j \leq u + (k)j = 0, 1, \dots, M-1 \quad (13)$$

$$\Delta u - (k) \leq \Delta u(k+j) \leq \Delta u + (k)j = 0, 1, \dots, M-1 \quad (14)$$

The Equations (13) and (14) represent the hard constraints for the optimization problem. MPC predicts the change in output system caused by the change in input system and solves an optimization problem at each time-step in order to calculate the actions that control the predicted plant output as close to the desired reference as possible. The main characteristic of MPC is predicting the future behavior of the controlled variables over predefined horizons. At each sampling interval, the real-time variations are measured and used to generate a new sequence of optimal actuation. Reference should be given to MPC to compute the value of cost function, where reference always represents the control

target. The predicted output is compared with the reference value and a residue (future error) is fed to the optimizer. The optimizer is based on the steady-state model of the process and is typically a linear model used to maximize a profit function and production rate and minimize a cost function. The optimal value of set point changes frequently due to the varying processed condition [28].

#### 4. Simulations and Result Analysis

In this paper, MPC is compared with some recently used evolutionary techniques. The latest evolutionary techniques used to mitigate LFC problem are the GA and FA.

GA is based on probabilistic search based on the population genetics. It starts with the candidates known as chromosomes. These chromosomes consist of genes, which are represented in terms of real or binary code. The environment of competition evolves new chromosomes. This evolution is achieved by three primary operations: Selection, crossover, and mutation. The evolutionary process helps the chromosomes to survive from one generation to another [13].

FA is also an algorithm for global optimization, which works on the behavior of fireflies. These flies belong to the family of insects, which attract the prey by its natural light. This light has an amazing pattern which usually attracts its prey. As the distance increases, the light intensity decreases, and this distance limits the communication between the fireflies. This algorithm is used to optimize the objective functions and has gained popularity by solving a wide range of real-world problems quite effectively [17]. FA not only has the ability to deal with multi-models, but also deals with non-linear optimization problems by dividing the population in chunks to make local attraction stronger over the long-distance attraction. Moreover, this algorithm has the ability to adapt any problem to control its modality. There are some rules used to define FA. It attracts other flies, irrespective to the composition. The brightness of FA will be determined by its objective function and the attraction decreases as distance increases. Therefore, FA depends on the attractiveness and variation in light.

The optimization function ( $J$ ) or objective function to tune the PI controller is given in Equation (15). In order to improve the response of the system, it is essential to minimize the objective function

$$J = \int_0^{\infty} t(|\Delta f_1| + |\Delta f_2| + |\Delta P_{tie}|)dt \quad (15)$$

where  $\Delta f_1$  is the change in frequency in area one and, similarly,  $\Delta f_2$  is the change in frequency in area two. Where  $\Delta P_{tie}$  is the power exchange between two areas. The parameters for GA and FA are formulated in Matlab to tune the PI controller.

First, the experiments are performed using GA and Fa, then MPC is used to compute the solution. The parameters used for GA for single/two areas are population size 50, crossover probability 0.8, maximum generation 100, and mutation probability 0.1. The tuning parameter for GA-PI are  $K_P = -0.5663$  and  $K_I = -0.4024$ , whereas, FA is set for 100 iterations with a population size of 50 for a single/two-area model. The tuning parameters for FA-PI are  $K_P = -0.8811$  and  $K_I = -0.5765$ . The parameters for MPC are set as prediction horizon 10, control horizon 2, sampling time 0.01sec, and weight on the output signal is 1. Moreover, the settling times are measured at  $\pm 2\%$  of the final state value for all the controllers. The robust analysis of the MPC for various certain load demands and its effect on mitigating the frequency fluctuation problem is elaborated in the upcoming sections.

##### 4.1. Design of Single-Area Model

Single-area model or system is generally used for low-demand purposes where the requirement of the load is low. In an interconnected system, a set of the PV and the thermal generator is called a single-area unit. The design of PV and thermal unit with its basic model is shown in Figure 4. The shown model uses MPC for optimization, and this same model with other controllers (GA-based PI, FA-based PI and PI) is used for experimentation and comparison of results.

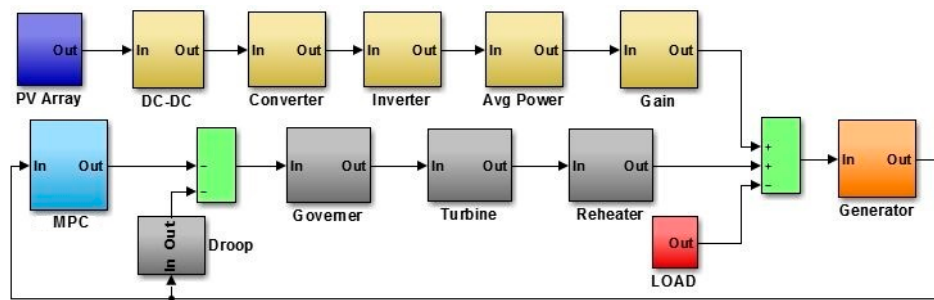


Figure 4. Single-area model using MPC-PI.

In this model, the PV array is connected via a number of stages and injects its power in the grid with a thermal unit that is fed to a generator whose feedback is passed through a droop and a controller to mitigate the frequency error.

Responses of different controllers on frequency fluctuation at 10% load change can be compared using Figure 5a, where PI controller has more frequency fluctuation as compared to other controllers. The controllers (FA, GA) show more oscillation than MPC. Figure 5b shows the response of the controllers when the load is changed from 10% to 20%. It is cleared from the response that the MPC has an extremely small change in its behavior. Moreover, PI controller shows the worst response, as it adds more oscillations when compared to other controllers. The worst-case scenario of frequency fluctuation is at 50% load change as shown in Figure 5c. However, this worst-case occurs rarely. MPC has a minor change in its response in terms of oscillation and FA gives a better response than GA for the worst test case.

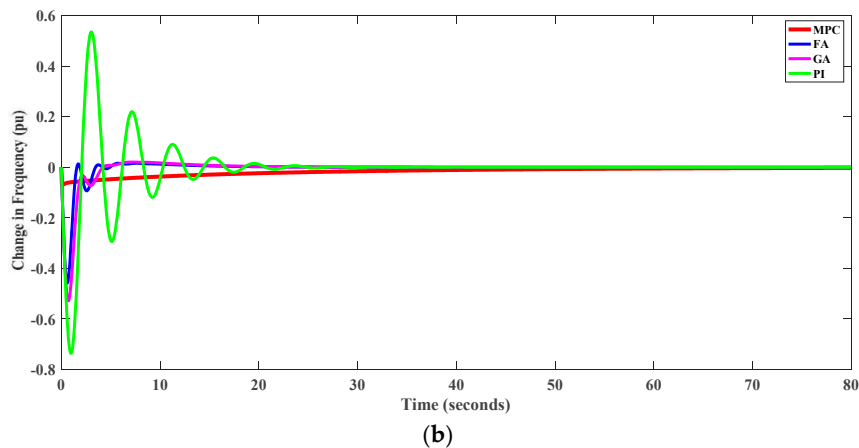
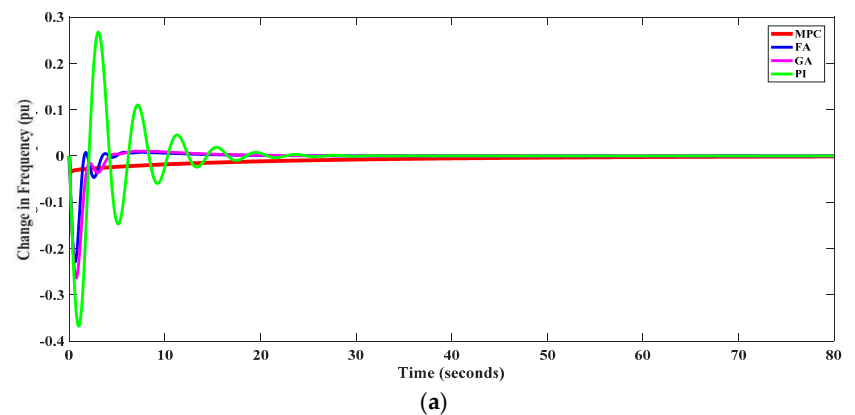


Figure 5. Cont.

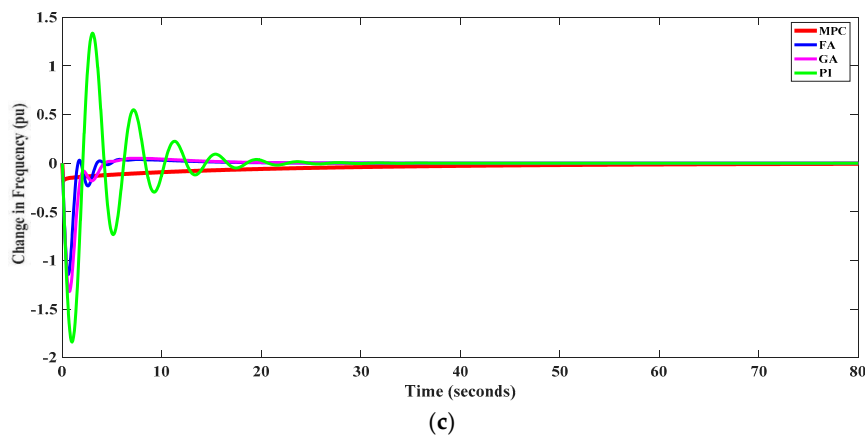


Figure 5. Single-area frequency response at: (a) 10% load change; (b) 20% load change; (c) 50% load change.

Table 3 lists the comparison of all controllers (MPC, FA, GA, PI) for different responses (steady state, undershoot, and overshoot) at 10%, 20%, and 50% load change. In all these cases, the best response in term of the specification is achieved using MPC which outperformed all other controllers and showed zero overshoot for the all the given load changing cases.

Table 3. The response time of controllers for the single-area model.

Specification	MPC			FA			GA			PI		
	10%	20%	50%	10%	20%	50%	10%	20%	50%	10%	20%	50%
Steady Time	7.43	15.07	20.3	6.08	9.67	12.59	6.98	10.65	14.74	15.38	17.31	22.40
Undershoot	0.03	0.04	0.13	0.23	0.45	1.15	0.26	0.52	1.32	0.36	0.73	1.84
Overshoot	0	0	0	0.01	0.02	0.03	0.01	0.02	0.05	0.37	0.53	1.33

#### 4.2. Design of Two-Area Model

A multi-area system offers benefits over a single-area system because of its capability to interchange and schedule power between different neighboring areas. In this paper, the two-area system is designed which contains a set of two units of PV and thermal generator each, where these units are interconnected via a transmission line (tie-line) for power exchange, as shown in Figure 6.

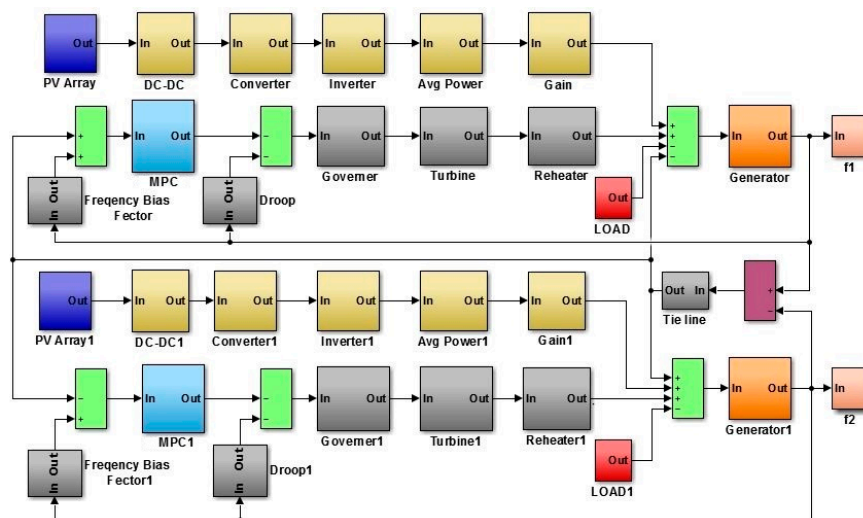


Figure 6. Two-area model using MPC.

On the bases of area control error (ACE), MPC will formulate to predict the future output. Where ACE indicates the mismatch in power between load and generation and can be expressed as Equation (16)

$$ACE = B\Delta\omega + \Delta P_{tie} \tag{16}$$

where  $B_i$  represents the bias factor which represents the disturbance in the load,  $\Delta\omega_i$  represent the change in frequency and  $\Delta P_{tie}$  represent power flow between different areas.

The response of two-area model on frequency fluctuation at 10% load change at field one (f1) is shown in Figure 7a. In this case, PI controller shows large settling time with less undershoot as compared to FA-based PI and GA-based PI. MPC shows minute fluctuation and no overshoot, which clearly negates the possibility of imbalance in the system. Figure 7b illustrates that the PI shows more oscillation as compared to the single-area, and FA shows less undershoot as compared to the GA, while MPC strictly follows its previous behavior. Furthermore, the oscillation in frequency for the worst-case scenario (improbable) and responses of all controllers can be compared using Figure 7c, where proposed MPC is not affected significantly by the load change, while other controllers show inefficiency and are badly affected by the load variation.

Table 4 presents and compares the response specifications of all the controllers under different load changing conditions. In all these cases, the percentage load change directly affects and increases the steady state, undershoot and overshoot errors. The best response among all the controllers in term of the specification is achieved using only MPC, which shows zero overshoot for the all the given load changing cases.

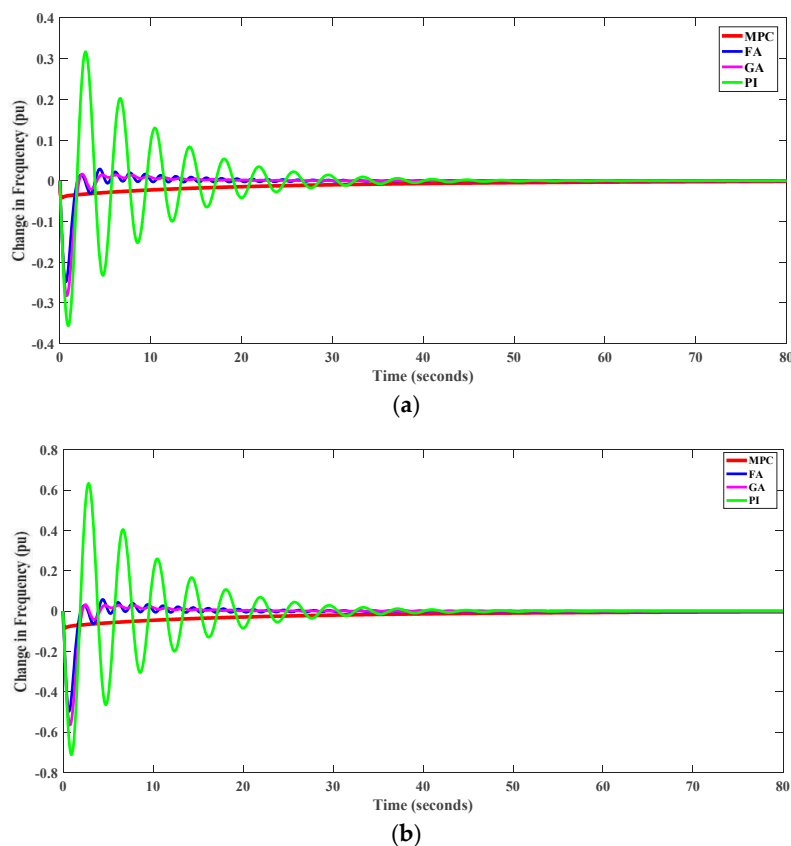
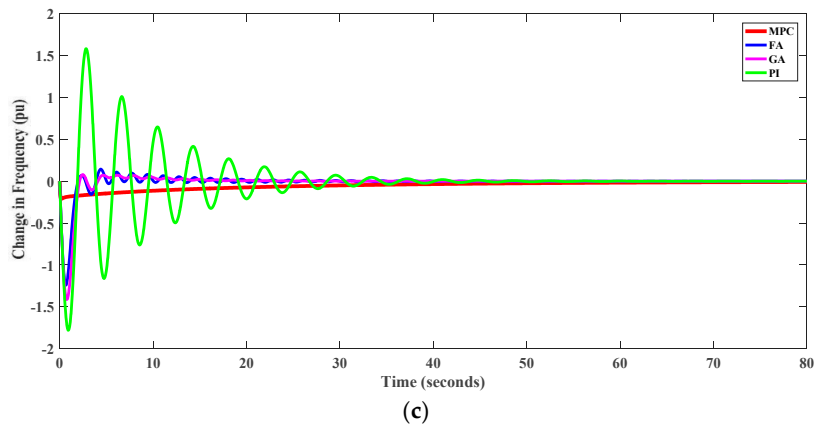


Figure 7. Cont.



**Figure 7.** Two-area frequency response at f1: (a) 10% load change; (b) 20% load change; (c) 50% load change.

**Table 4.** The response time of controllers for f1 in the two-area model.

Specification	MPC			FA			GA			PI		
	10%	20%	50%	10%	20%	50%	10%	20%	50%	10%	20%	50%
Steady Time	12.64	24.69	29.52	11.81	13.71	20.39	10.74	12.38	16.17	25.94	31.59	37.68
Undershoot	0.03	0.07	0.18	0.25	0.52	1.24	0.28	0.56	1.41	0.35	0.70	1.73
Overshoot	0	0	0	0.02	0.08	0.14	0.01	0.02	0.07	0.33	0.65	1.62

The responses of all controller on frequency fluctuation at 10% load change for field two (f2) can be visualized using Figure 8a.

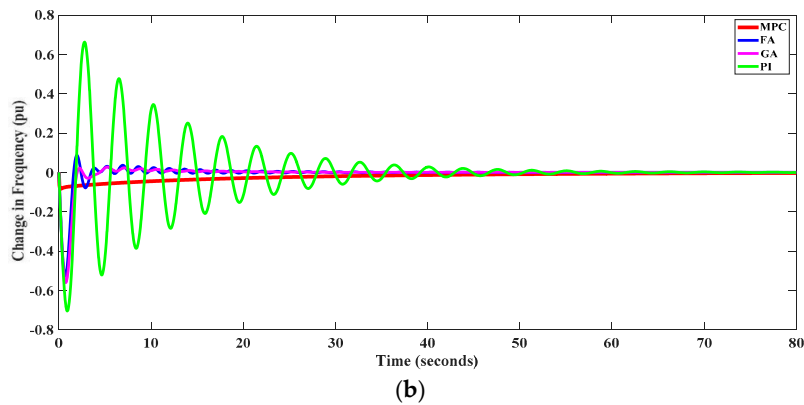
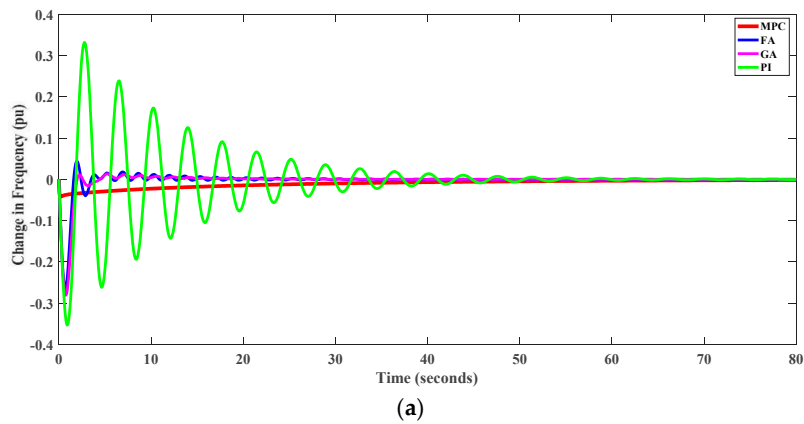


**Figure 8.** Cont.

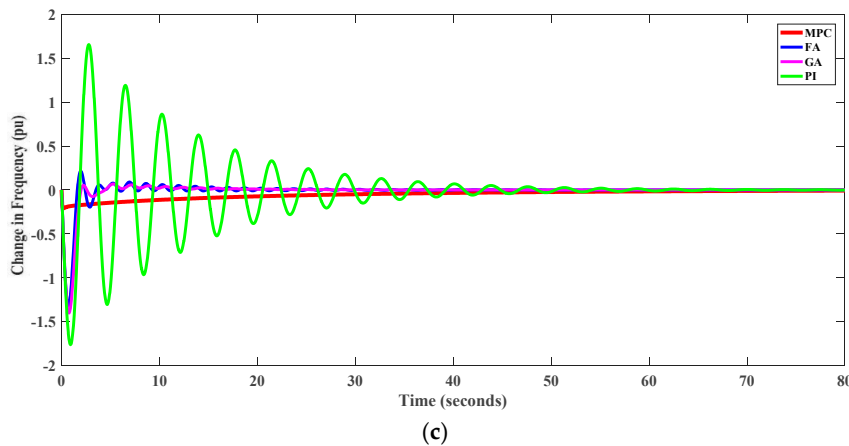


**Figure 8.** Two-area frequency response at f2: (a) 10% load change; (b) 20% load change; (c) 50% load change.

PI controller has large settling time with less undershoot, but the response time of MPC is robust as compared to GA and FA, where these controllers are showing more oscillations. In Figure 8b, the fluctuation of frequency at 20% load change is analyzed, where MPC strictly follow its specifications irrespective to variation in load. The worst-case scenario, at 50% load change, is shown in Figure 8c. MPC maintained its reputation even for the worst case, while other controllers were unable to consolidate this fluctuation problem.

Table 5 presents the comparison of different response specifications for all the controllers for f2 in the two-area model. Again, it can be seen that the best response among all the controllers in term of the specification is achieved using the MPC, which showed minimum oscillation for all the given load changing cases.

**Table 5.** The response time of controllers for f2 in the two-area model.

Specification	MPC			FA			GA			PI		
	10%	20%	50%	10%	20%	50%	10%	20%	50%	10%	20%	50%
Steady Time	16.07	19.68	25.29	11.07	14.40	19.31	10.93	11.70	17.27	30.62	34.84	42.05
Undershoot	0.04	0.08	0.20	0.26	0.52	1.32	2.28	0.56	0.14	0.35	0.71	1.75
Overshoot	0	0	0	0.04	0.08	0.21	0.01	0.02	0.07	0.33	0.67	1.68

### 4.3. Design of Tie-Power Line

Figure 9 shows the scheduling of power between two areas on 10%, 20%, and 50% load changing conditions. It is preferable that a change in tie-power ( $\Delta P$  tie) should be minute. In all cases, although the response of PI is much better than the GA and FA controllers, there are still some oscillations before the system gains a constant value. Moreover, the GA gives minimum overshoot, but it possesses the maximum undershoot, while the FA is having maximum overshoot. The response of MPC shows the rapid transfer of power with minimum oscillations, while all other controllers are unable to follow the required specifications of  $\Delta P$  tie. Even for the worst-case scenario of deviation in power at 50% load change, MPC maintains its fame with minimum fluctuation.

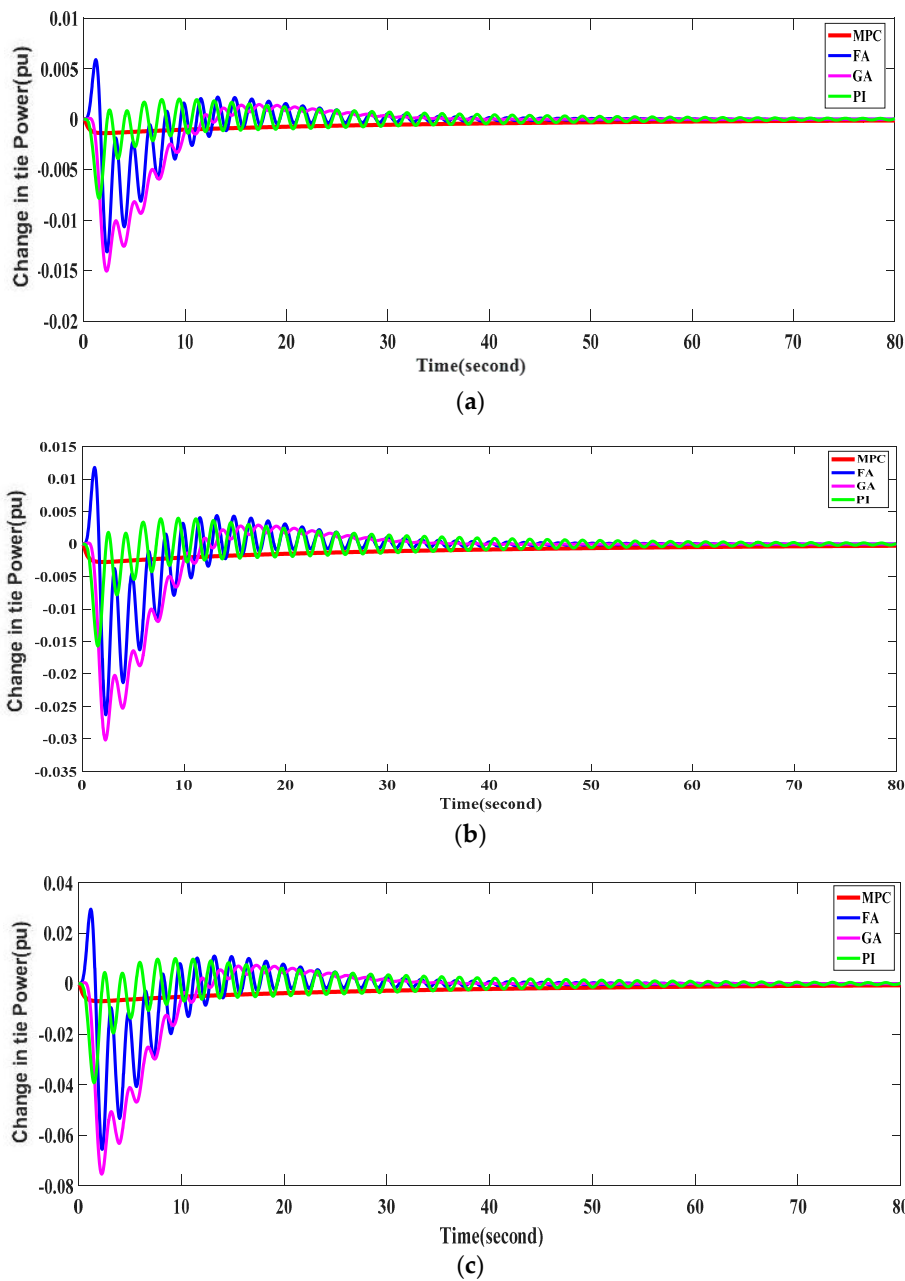


Figure 9. Deviation in tie-power at: (a) 10% load change; (b) 20% load change; (c) 50% load change.

The scheduling of power between different areas and responses of all controllers on power exchange can be analyzed using Table 6. The MPC interchanges the power more comprehensively and shows minimum oscillation for all the given load changing conditions in comparison to other controllers.

Table 6. The response time of controllers for the tie-power two-area model.

Specification	MPC			FA			GA			PI		
	10%	20%	50%	10%	20%	50%	10%	20%	50%	10%	20%	50%
Steady Time	7.18	8.31	10.17	30.91	32.51	37.49	30.09	31.98	35.31	39.51	41.85	50.20
Undershoot	0.032	0.003	0.007	0.013	0.026	0.066	0.015	0.030	0.074	0.008	0.002	0.04
Overshoot	0	0	0	0.01	0.02	0.03	0.001	0.002	0.007	0.02	0.04	0.01

#### 4.4. Multiple Load Changing Conditions

Figure 10 is representing the single area response under certain variation in load. As load does not remain constant and varies with the passage of time, the frequency fluctuation is analyzed at different loads (10%, 50%, 20%, 10%, 15%), and the mitigating ability of controllers are analyzed where MPC shows its superiority to tackle rapid variation in load. However other controllers GA, FA, and PI show more oscillations.

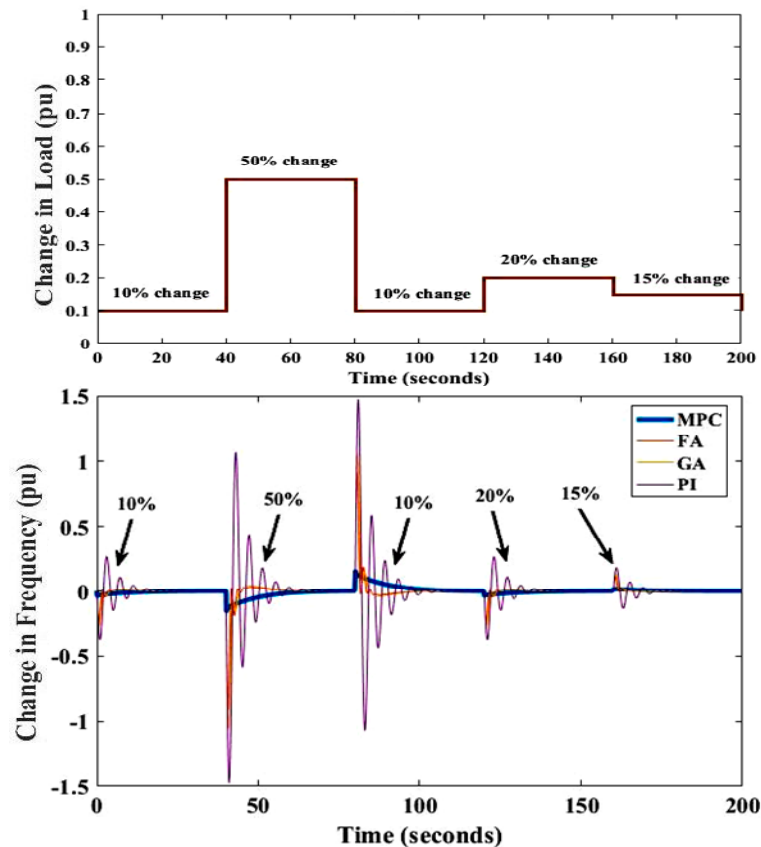


Figure 10. Frequency Fluctuations for Single Area with different load changing conditions.

Figures 11 and 12 depict two area responses on realistically based scenarios where load does not remain constant. Under certain changes in load, the frequency deteriorates, and adverse effects arise when there is 50% change in load. The frequency shows aggressive spikes and it takes some time to settle even the load has been changed to 10% or around 15%. However, MPC maintains its reputation and handles the frequency variation in an impressive way, while other controllers are unable to compete with MPC fluctuation handling capabilities.

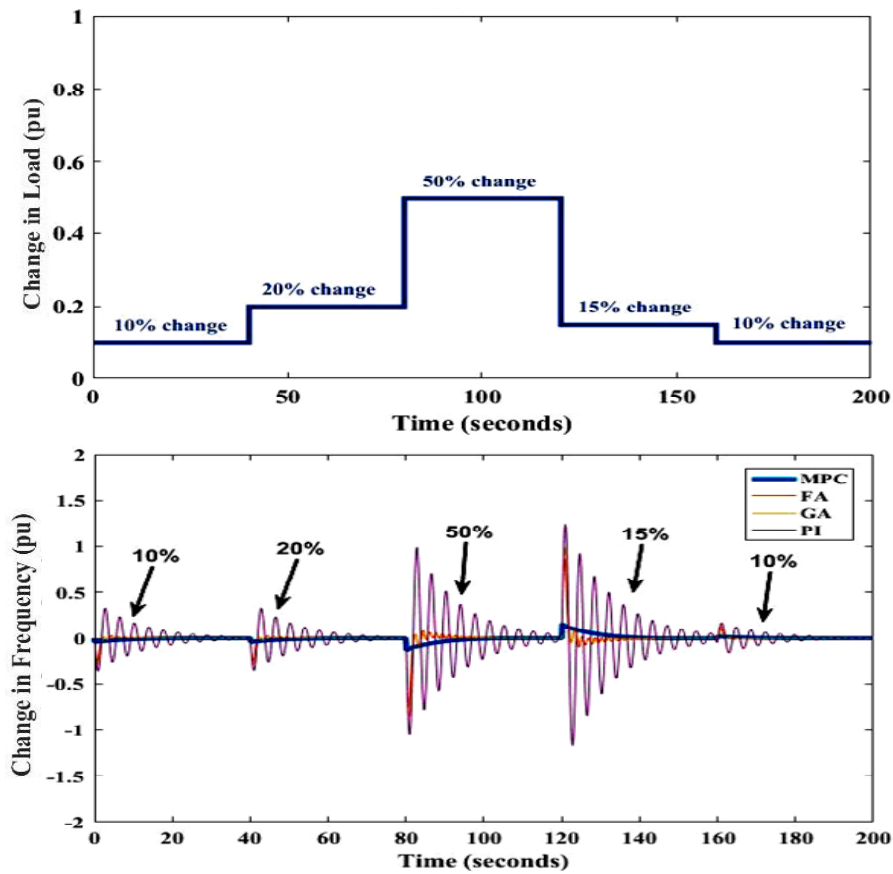


Figure 11. Frequency Fluctuations for Two Area at f1 with different load changing conditions.

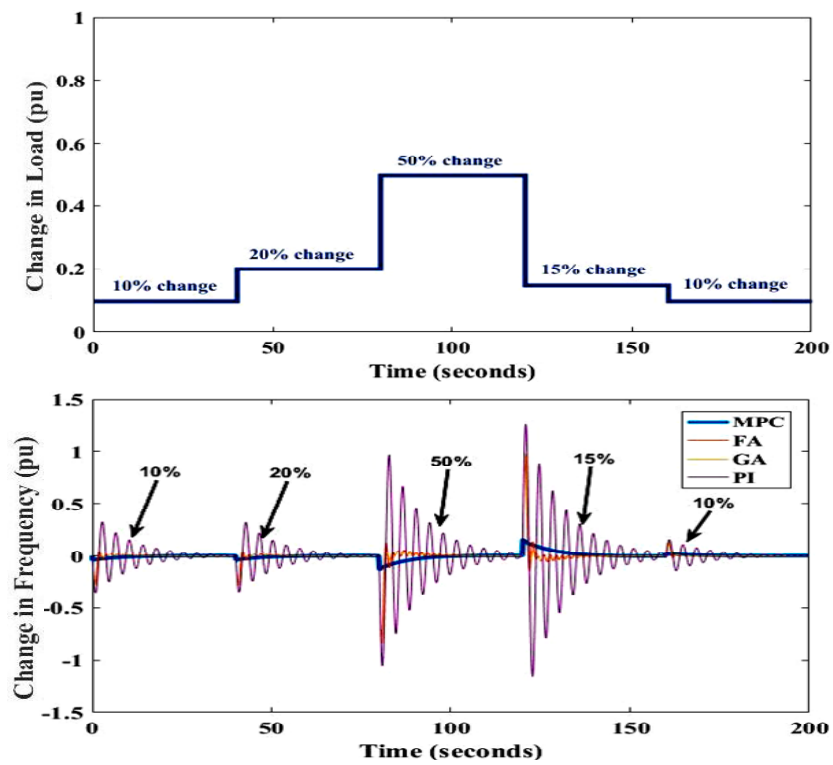


Figure 12. Frequency Fluctuations for Two Area at f2 with different load changing conditions.

In Figure 13 the tie-line power exchange is also monitored with a random change in load. The two-area power exchange with the robustness of MPC can be seen where the exchange of power between the areas is rapid as compared to other controllers.

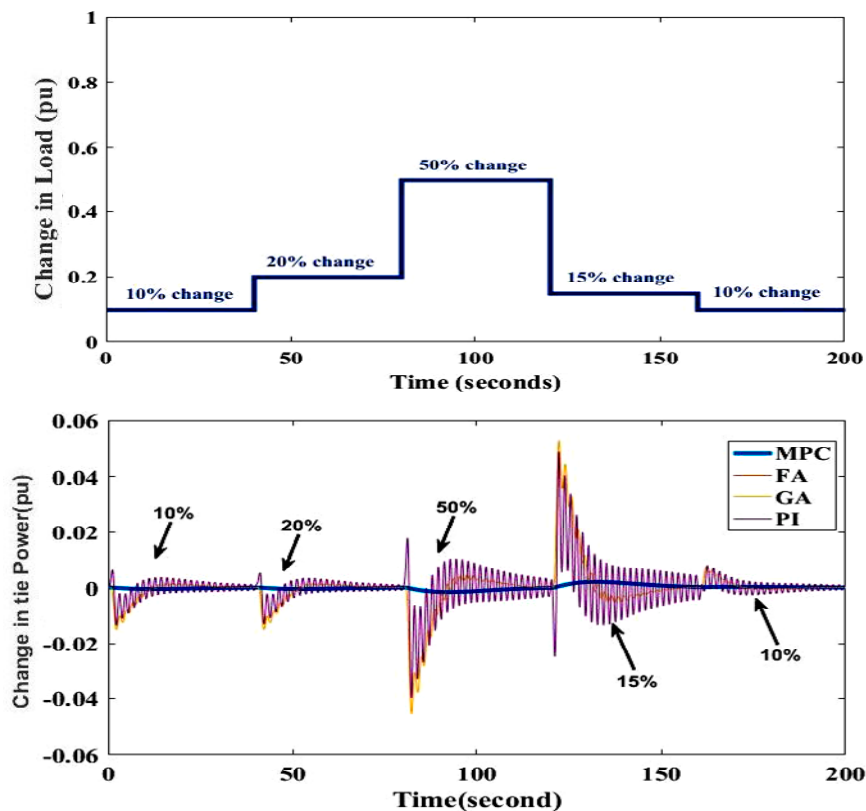


Figure 13. Frequency fluctuations for tie-power with different load changing conditions.

## 5. Conclusions

In this paper, the problem of LFC due to load change is analyzed and the problem is mitigated by introducing MPC in the system. The results are observed and analyzed on realistically based scenarios, where load does not remain constant at 10%, 15%, 20%, and even for the worst-case scenario of 50% load change. Moreover, the PV connected thermal grid system with a tie-line was developed, and transmission line power is observed where the objective function was to improve the overall response of the system. It is concluded from the results that MPC is robust, tracks its optimal value in an efficient way irrespective to the load change, and outperforms all other discussed controllers for a single/two-area system in term of undershoot, overshoot, and oscillation.

**Author Contributions:** All authors contributed equally to this work.

**Funding:** This research received no external funding.

**Conflicts of Interest:** The authors declare no conflict of interest.

## References

1. Das, S.; Akella, A.K. Power Flow Control of PV-Wind-Battery Hybrid Renewable Energy Systems for Stand-Alone Application. *Int. J. Renew. Energy Res.* **2018**, *8*, 36–43.
2. Tedesco, F.; Casavola, A. Fault-tolerant distributed load/frequency supervisory strategies for networked multi-area microgrids. *Int. J. Robust Nonlinear Control* **2014**, *24*, 1380–1402. [[CrossRef](#)]
3. Kumar, K.A.; Selvan, M.P.; Rajapandiyam, K. Dynamic grid support system for mitigation of impact of high penetration solar PV into grid. In Proceedings of the 2017 7th International Conference on Power Systems (ICPS), Pune, India, 21–23 December 2017; pp. 646–652. [[CrossRef](#)]

4. Samadi, A.; Soder, L.; Shayesteh, E.; Eriksson, R. Static Equivalent of Distribution Grids With High Penetration of PV Systems. *IEEE Trans. Smart Grid* **2015**, *6*, 1763–1774. [[CrossRef](#)]
5. *REN21 Renewables 2018 Global Status Report*; REN21: Paris, France, 2018.
6. Sahu, R.K.; Panda, S.; Padhan, S. A novel hybrid gravitational search and pattern search algorithm for load frequency control of nonlinear power system. *Appl. Soft Comput. J.* **2015**, *29*, 310–327. [[CrossRef](#)]
7. Arlene Davidson, R.; Ushakumari, S. Optimal load frequency controller for a deregulated non-reheat thermal power system. In Proceedings of the 2015 International Conference on Control Communication & Computing India (ICCC), Trivandrum, India, 19–21 November 2015; pp. 319–324. [[CrossRef](#)]
8. Taher, S.A.; Hajiakbari Fini, M.; Falahati Aliabadi, S. Fractional order PID controller design for LFC in electric power systems using imperialist competitive algorithm. *Ain Shams Eng. J.* **2014**, *5*, 121–135. [[CrossRef](#)]
9. Vrdoljak, K.; Perić, N.; Petrović, I. Sliding mode based load-frequency control in power systems. *Electr. Power Syst. Res.* **2010**, *80*, 514–527. [[CrossRef](#)]
10. Sundaram, V.S.; Jayabarathi, T. Load Frequency Control using PID tuned ANN controller in power system. In Proceedings of the 2011 1st International Conference on Electrical Energy Systems, Newport Beach, CA, USA, 3–5 January 2011; pp. 269–274. [[CrossRef](#)]
11. Patel, N.; Bhusan Jain, P. Automatic Generation Control of Three Area Power Systems Using Ann Controllers. *Int. J. Comput. Eng. Res.* **2013**, *3*, 1–7.
12. Bevrani, H.; Daneshmand, P.R. Fuzzy Logic-Based Load-Frequency Control Concerning High Penetration of Wind Turbines. *IEEE Syst. J.* **2012**, *6*, 173–180. [[CrossRef](#)]
13. Yousef, H. Adaptive fuzzy logic load frequency control of multi-area power system. *Int. J. Electr. Power Energy Syst.* **2015**, *68*, 384–395. [[CrossRef](#)]
14. Ali, E.S.; Abd-Elazim, S.M. Bacteria foraging optimization algorithm based load frequency controller for interconnected power system. *Int. J. Electr. Power Energy Syst.* **2011**, *33*, 633–638. [[CrossRef](#)]
15. Daneshfar, F.; Bevrani, H. Multiobjective design of load frequency control using genetic algorithms. *Int. J. Electr. Power Energy Syst.* **2012**, *42*, 257–263. [[CrossRef](#)]
16. Soundarrajan, A.; Sumathi, S.; Sundar, C. Particle swarm optimization based LFC and AVR of autonomous power generating system. *IAENG Int. J. Comput. Sci.* **2010**, *37*, 85–92.
17. Omar, M.; Soliman, M.; Abdel Ghany, A.M.; Bendary, F. Optimal tuning of PID controllers for hydrothermal load frequency control using Ant Colony Optimization. *Int. J. Electr. Eng. Inform.* **2013**, *5*, 348–360. [[CrossRef](#)]
18. Abd-Elazim, S.M.; Ali, E.S. Firefly algorithm-based load frequency controller design of a two area system composing of PV grid and thermal generator. *Electr. Eng.* **2018**, *100*, 1253–1262. [[CrossRef](#)]
19. Abdelaziz, A.Y.; Ali, E.S. Load frequency controller design via artificial cuckoo search algorithm. *Electr. Power Compon. Syst.* **2016**, *44*, 90–98. [[CrossRef](#)]
20. Yuniahastuti, I.T.; Anshori, I.; Robandi, I. Load frequency control (LFC) of micro-hydro power plant with capacitive energy storage (CES) using bat algorithm (BA). In Proceedings of the 2016 International Seminar on Application for Technology of Information and Communication (ISemantic), Semarang, Indonesia, 5–6 August 2016; pp. 147–151. [[CrossRef](#)]
21. Ma, M.; Chen, H.; Liu, X.; Allgöwer, F. Electrical Power and Energy Systems Distributed model predictive load frequency control of multi-area interconnected power system. *Int. J. Electr. Power Energy Syst.* **2014**, *62*, 289–298. [[CrossRef](#)]
22. Pandey, S.K.; Mohanty, S.R.; Kishor, N. A literature survey on load-frequency control for conventional and distribution generation power systems. *Renew. Sustain. Energy Rev.* **2013**, *25*, 318–334. [[CrossRef](#)]
23. Santy, T.; Natesan, R. Load Frequency Control of a Two Area System Consisting of a Grid Connected PV System and Diesel Generator. *Int. J. Emerg. Technol. Comput. Sci. Electron.* **2015**, *13*, 456–461.
24. Javed, M.Y.; Murtaza, A.F.; Ling, Q.; Qamar, S.; Gulzar, M.M. A Novel MPPT design using Generalized Pattern Search for Partial Shading. *Energy Build.* **2016**, *133*, 59–69. [[CrossRef](#)]
25. Mohamed, T.H.; Bevrani, H.; Hassan, A.A.; Hiyama, T. Decentralized model predictive based load frequency control in an interconnected power system. *Energy Convers. Manag.* **2011**, *52*, 1208–1214. [[CrossRef](#)]
26. Mohamed, T.H.; Morel, J.; Bevrani, H.; Hiyama, T. Model predictive based load frequency control-design concerning wind turbines. *Int. J. Electr. Power Energy Syst.* **2012**, *43*, 859–867. [[CrossRef](#)]

27. Ersdal, A.M.; Imslund, L.; Uhlen, K. Model Predictive Load-Frequency Control. *IEEE Trans. Power Syst.* **2016**, *31*, 777–785. [[CrossRef](#)]
28. Shi, X.; Hu, J.; Yu, J.; Yong, T.; Cao, J. A novel load frequency control strategy based on model predictive control. In Proceedings of the 2015 IEEE Power & Energy Society General Meeting, Denver, CO, USA, 26–30 July 2015. [[CrossRef](#)]



© 2019 by the authors. Licensee MDPI, Basel, Switzerland. This article is an open access article distributed under the terms and conditions of the Creative Commons Attribution (CC BY) license (<http://creativecommons.org/licenses/by/4.0/>).